Available at www.ijcasonline.com **ISSN:2349 – 0594**

International Journal of Modern Chemistry and Applied Science

International Journal of Modern Chemistry and Applied Science, 2017, 4(4),561-567

Synthesis, Characterization of $ZrO_2/Fe_2O_3/Al_2O_3$ Ternary Nanocomposite for Photocatalytic degradation of Congo red dye from aqueous solution

Kasahun Chala Bayisa*

College of Natural and computational Sciences, Departmentof Chemistry, Dilla University, Ethiopia

Abstract: The objective of this study was to investigate adsorption efficiency of $ZrO_2/Fe_2O_3/Al_2O_3$ ternary mixed oxide nanoparticle for photocatalytic-degradation of Congo red from aqueous solution. For this purpose, the adsorbent was synthesized by sol-gel method. The surface structure of the as-synthesized material was investigated by means of XRD, SEM-EDXand FT-IR to understand the effect of surface properties on the photocatalytic-degradation behavior of this particular organic pollutant.The band gap energy of the $ZrO_2/Fe_2O_3/Al_2O_3$ photocatalyst was calculated to be 2.267 eV this indicated that the as-synthesize sample had high photo-absorption property in the visible light region.Experimental result of the $ZrO_2/Fe_2O_3/Al_2O_3$ photocatalyst calcined at 700°C in 180 min at percentage compositions of Zr, Fe, and Al were 50, 35 and 5, respectively, exhibited high photocatalytic activity of 97.7% under visible light irradiation.The pseudo-first-order rate constants of CR dye degradation in the presence of the catalyst were calculated as 8.3×10^{-3} and 1.66×10^{-2} min^{-1} under UV and visible light irradiation, respectively. In all the conditions studied, the pseudo- first-order equation did fit well to the whole range of contact times.

Keywords: Congo red, nanoparticle, photocatalytic-degradation, sol-gel synthesis, ternary oxide.

1 Introduction

Most dyes used in the pigmentation of textiles, paper, leather, ceramics, cosmetics, inks and food processing products are derived from azo dyes, which are characterized by the presence of one or more azo groups (-N=N-) in their structure [1]. Approximately 15% of the dyes produced worldwide are lost within waste water during synthesis and processing [2]. This waste represents a great hazard to human and environmental health due to the toxicity of azo dyes [3].In order to remove hazardous materials like toxic organic and inorganic substances from wastewater is very difficult [4-5]. There are various methods for removal of organic and inorganic compounds from the wastewater as filtration, electrolysis, precipitation, ion exchange and adsorption process [6]. Most of these methods require high capital and recurring expenditure and consequently they are not suitable for small scale industries [7]. However, heterogeneous photo-catalysis on semiconductors has become an alternative treatment method for degradation of organic pollutants from wastewater which has the ability to mineralize organic compounds. Solar energy, an abundant natural energy source, can be widely utilized in the photo-catalytic degradation of pollutants.

The semiconducting metal oxides like iron oxide (Fe_2O_3) nanomaterials exhibit promising photocatalytic activities due to their environmental friendly behavior, low catalyst cost, high specific surface area, high crystallinity and solar energy application [8–10] and thus, could be an alternative material for environmental application and wastewater treatment [11–13]. Alumina (Al_2O_3) is one of the most widely used ceramics due to its high specific surface area, very good thermal stability and amphoteric properties [14]. Due to these characteristics porous alumina is generally a very good candidate as a catalyst carrier as well as an adsorbent.

Zirconium oxide (ZrO_2) nanoparticle has face centered-cubic crystalline structure in which each tetravalent metal ion is surrounded by eight equivalents nearest O^{2-} ions forming the vertices of a cube. This structure renders zirconia high oxygen vacancy concentration and mobility properties [15]. Such zirconia also possesses unique bi-functional characteristics of weak acidic and basic properties [16] as well as high thermal stability under reducing or oxidizing atmospheres. Thus zirconia has been extensively investigated as a robust catalyst, catalyst promoter or support. Fine particle zirconia bears the better wear resistance [17] and lower diffusion resistance, which are favorable for catalyst applications. In addition, nanocrystalline zirconia having higher adsorptive capacity thus appears promising for adsorption applications.

In this study, I prepared ternary mixed oxide $ZrO_2/Fe_2O_3/Al_2O_3$ nanocomposite using sol-gel method. Here mixing of two or more metal oxide phases can be controlled on both the molecular and the nanoscale. This ternary mixed oxide photocatalyst has high adsorption capacity among binary nanoparticles and attractive with respect to applications in photocatalysis due to its high specific surface area, crystallinity, photochemical stability, ability to disintegrate water molecule into hydrogen and hydroxide ions and a new generation environmental friendly photocatalyst. I also studied the effect of additives on the kinetics and the mechanism of photocatalytic degradation of the CR dye.

2 Materials and methods

2.1 Synthesis of photocatalyst

The $ZrO_2/Fe_2O_3/Al_2O_3$ photocatalyst was synthesized by the sol-gel method using zirconium, iron and aluminum nitrates solution in the presence of ethanol, distilled water

and nitric acid solution at volume ratio of 4:3:1 respectively. In this regard, a precursorcomposition of 50-35-5 of $ZrO_2/Fe_2O_3/Al_2O_3$ was prepared from 16.06 gram $ZrO(NO_3)_2.5H_2O$ (Aldrich) was dissolved in 20 ml ethanol, 1.8 ml water and 0.6 ml nitric acid. Simultaneously 14.14 gram $Fe(NO_3)_3.9H_2O$ (Merck), and 1.875 gram $Al(NO_3)_3.9H_2O$ (Merck) solution were mixed to zirconium solution through stirring and the pH level was adjusted to ~9 using aqueous ammonia. The obtained mixture heated at 80^{o}C with continuous stirring for 2 hrs and cooled at room temperature. The sample was further calcined at 700 and 800^{o}C for 3 hrs in the muffle furnace. Finally, the as synthesized photocatalyst was characterized by XRD (Bruker D8), SEM-EDAX, FTIR(Bruker Optics EQUINOX 65) and measured UV-Vis absorbance from 200-800 nmusing (NV 203) spectrophotometer for the estimation of band gap absorption edge of the as-synthesized photocatalyst.

2.2 Photocatalyticdegradation experiment

The photocatalytic study of mixed oxide $ZrO_2/Fe_2O_3/Al_2O_3$ ternary nanocomposite both sintered and unsintered sample was carried out by taking 5 mg photocatalyst powder sample into 100 ml of Congo red ($C_{32}H_{22}N_6O_6S_2Na_2$) solution (50 mgL^{-1}) under stirring condition. Then, to establish the adsorption equilibrium between the CR and the photocatalyst, the resulting solution was stirred in the dark for 20 min. The zero time reading was taken atλ_{max} (547 nm) and the solution was exposed to a xenon lamp. After appropriate time of stirring, the solution was filtered by whatman-40 filter paper and finally analyzed by UV-Visible spectrophotometer (NV 203) at 20 minute time intervals for 180 min was measured.

3 Result and discussion

3.1 Photocatalyst powder study

3.1.1 XRD Analysis

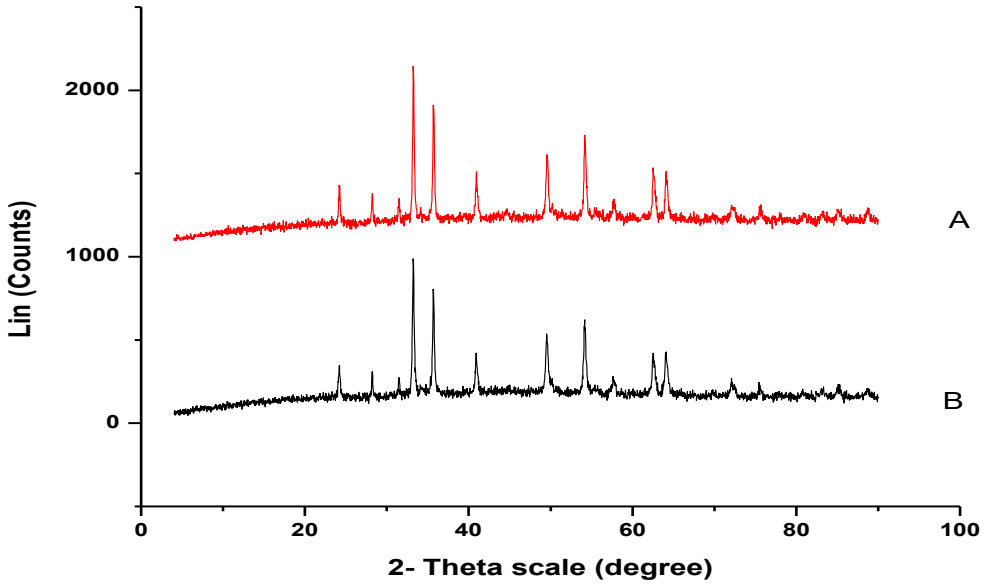

Figure1: XRD pattern of $ZrO_2/Fe_2O_3/Al_2O_3$ photocatalyst powder calcined at 800^{o}C (A) and 700^{o}C (B).

XRD pattern of as-synthesized $ZrO_2/Fe_2O_3/Al_2O_3$photocatalyst powder in figure 1(a),1(b),after calcination processes, exhibits well crystallization of monoclinic and stabilized tetragonal zirconia, α-Al_2O_3 and Fe_2O_3 phases. The diffraction peaks at 2θ = 35.90° is corresponding to iron oxide phase at 2θ = 40.24°, 62.53° and 64.36° are corresponding to alumina and that at 2θ = 26.71° corresponding to tetragonal (t) zirconia. According to the estimations performed using the Scherer method [18],

$$D_s = \frac{0.9\lambda}{\beta \cos\theta} \quad \ldots\ldots\ldots\ldots\ldots\ldots (1)$$

The crystallite sizes of the t- ZrO_2, Fe_2O_3 and Al_2O_3 phases were 21, 17.5 and 14.3 nm, respectively. It is known that at room temperature, ZrO_2 has three polymorphs of monoclinic (m), tetragonal (t) and cubic (c) crystal structures, with m-zirconia equilibrium bulk structure [19–21]. This study clearly shows the effect of different foreign ionic species on the phase transformation behavior of zirconia. There are many studies available in literature regarding the phase transformation behavior of zirconia and Various attempts have been made to stabilize the c- or t-ZrO_2such as doping small amounts of different dopants such as Y_2O_3, MgO, CaO, Al_2O_3, etc. [22-24]; so that it can exist at room temperature.

The stabilization of the zirconia has also been demonstrated to be related to both the size effect [25] and the presence of aluminum ions on the surface of the zirconia particles [26]. The presence of tetragonal zirconia in the present study indicates that the crystallite size of pure ZrO_2 synthesized by sol-gel method is less than the critical size. In this work, the stabilization of t-zirconia phase in $ZrO_2/Fe_2O_3/Al_2O_3$ nanocomposites is believed to be attributed to both the size effect and the existence of Al^{3+} cations surrounding the zirconia particles. However, based on equation (1) the mixed oxide $ZrO_2/Fe_2O_3/Al_2O_3$ nanocomposite calcined at 700^{o}C and 800^{o}C has particle size 41.05 and 49.53 nm respectively. Accordingly, the ternary mixed oxide with the smallest size was found to exhibit the largest specific surface area[27].

3.1.2 FTIR Analysis

The FT-IR spectrum of the $ZrO_2/Fe_2O_3/Al_2O_3$ photocatalyst powder sample was carried out in KBr medium and the results obtained as such are depicted on figure (2) with the main absorption peaks located 3405, 2920, 1619,

535 and 463 cm^{-1}. Accordingly, the absorption peaks at the intense band of 3405 cm^{-1} may be due to the stretching modes of -OH group from adsorbed water in the sample. The band observed at 2920 cm^{-1} can be assigned to the bending vibration of free water molecule; while bands observed at 1619, 1382 and 1258 cm^{-1} may be attributed to -CH, $-CH_2$ and $-CH_3$ functional groups. The bands at 535 cm^{-1} and 463 cm^{-1} are assigned to the bending vibrations of the mixed metal oxide(M-O) and metal-metal oxides (M-M-O), respectively [28].

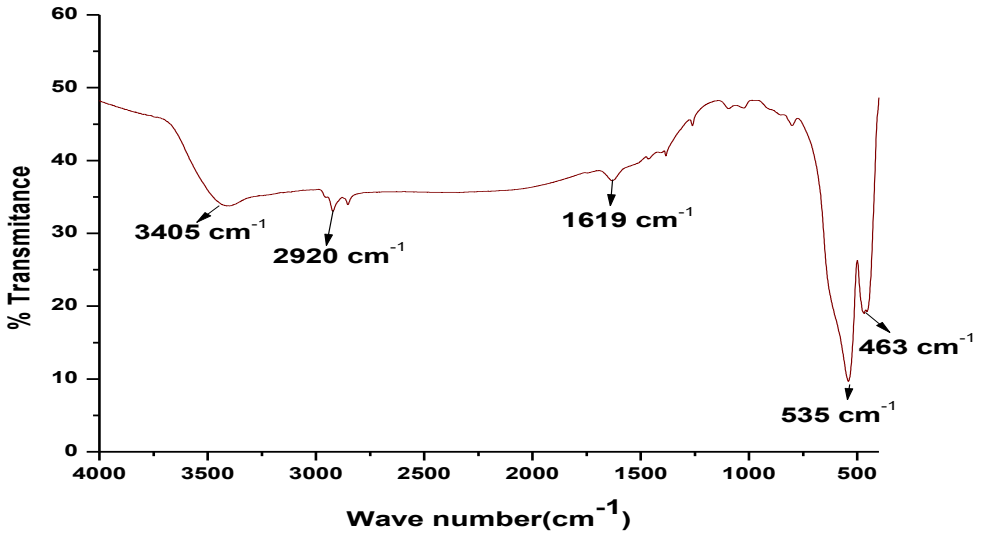

Figure 2: FTIR spectra of $ZrO_2/Fe_2O_3/Al_2O_3$ photocatalyst powder.

3.1.3 Scanning electron microscopy (SEM) study

The surface morphology of $ZrO_2/Fe_2O_3/Al_2O_3$ photocatalyst powder has been studied by scanning electron microscopy method. Figure (3)represents the SEM and EDAX images of mixed oxide $ZrO_2/Fe_2O_3/Al_2O_3$ nanocomposites prepared by sol-gel synthesis. There are numerous micro-pores present on the surface of the particles. These inter-particle pores are due to the escaping gases formed during the combustion process. The presences of zirconium (Zr), iron (Fe) and aluminum (Al) elements in the mixed composite were confirmed by the EDAX spectrum.

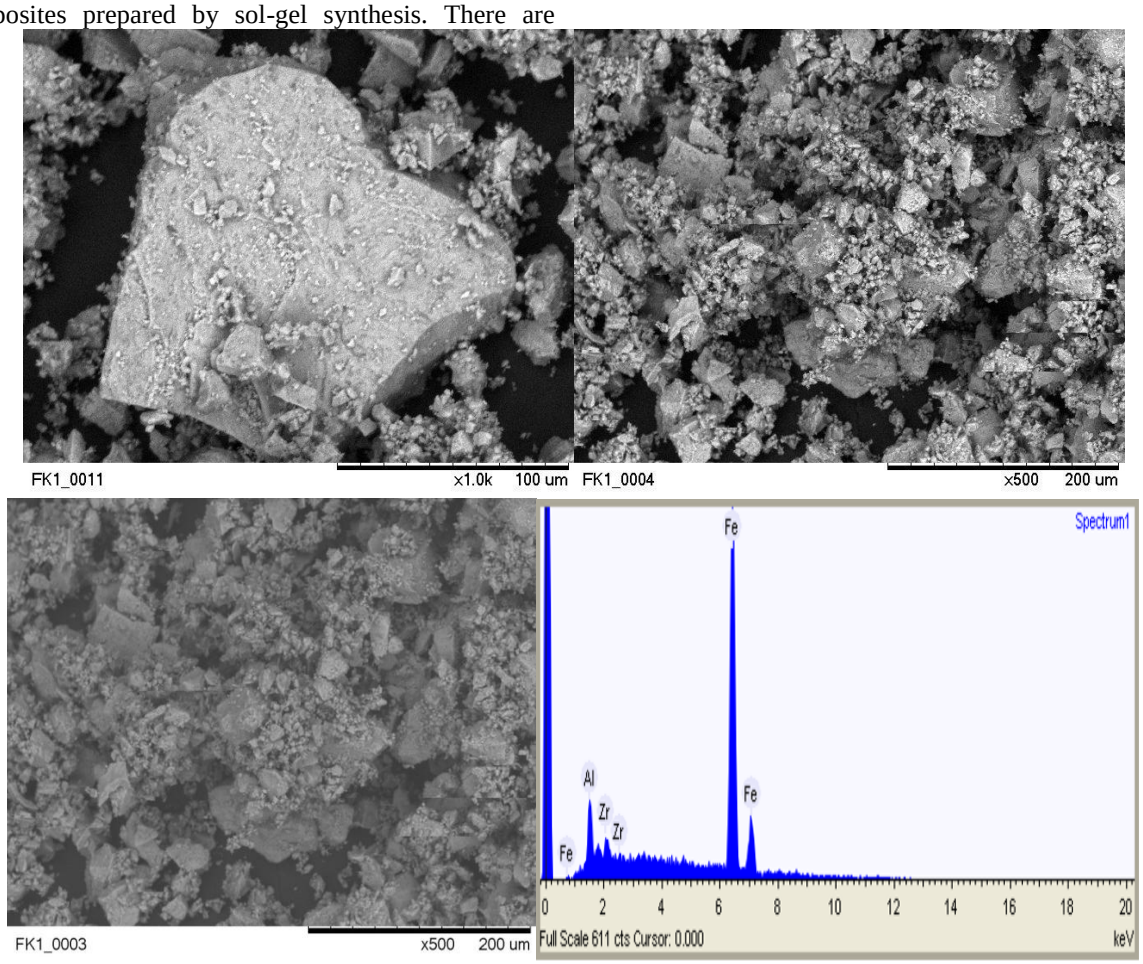

Figure 3: SEM and EDAX images of $ZrO_2/Fe_2O_3/Al_2O_3$ photocatalyst powder.

Table 1: Summary results of EDAX analysis

Elements	Weight (%)
Zirconium	**49.3**
Iron	**33.8**
Aluminum	**3.4**

The result indicated in (Table 1) that the percentage composition of Zr, Fe and Al in the as-synthesized photocatalyst was found to be 49.3, 33.8 and 3.4 respectively and this is not far from the theoretical composition of % (50-35-5)Zr, Fe and Al respectively.

3.1.4 Band gap energy determination

Since the absorption of light is related to the band gap, scanning of the absorption spectra of materials enables computation of the band gap. For this purpose, UV-Visible Spectrophotometer was used to record spectra of the as-synthesized $ZrO_2/Fe_2O_3/Al_2O_3$ photocatalystdissolved in ethanol. From this spectrum, the point of inflection between high transmittance and high absorption was identified. The wavelength corresponding to this point of inflection is termed as 'absorption edge or band edge' as shown in the figure(4)given below.

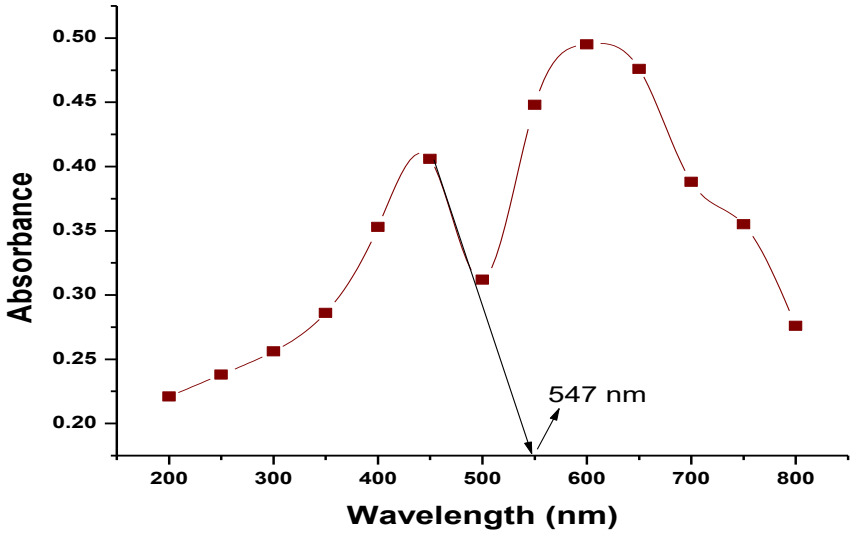

Figure 4: Uv-visible absorbance of $ZrO_2/Fe_2O_3/Al_2O_3$ photocatalyst.

The absorption edge of the samples was determined by the following equation[29],

$$Eg(eV) = \frac{1240}{\lambda} \text{..... (2)}$$

Where: E_g is band gap energy in electron volt, λ is wavelength (nm) corresponding to absorption edge.

From the UV/Visible spectrum of $ZrO_2/Fe_2O_3/Al_2O_3$ photocatalyst, the band gap energy was calculated using equation (2)is 2.267 eV at the band gap absorption edge of 547 nm. The monoclinic form ZrO_2 has two direct interband transitions at 5.93 eV and 5.17 eV, whereas the tetragonal form has a band gap of 5.1 eV [30]. As compared to the present study such a reduction in the band gap energy may be the presence of Fe_2O_3/Al_2O_3 in the zirconia matrix significantly modifies the UV absorption feature of the zirconium dioxide. Therefore, the result indicates that the $ZrO_2/Fe_2O_3/Al_2O_3$photocatalyst powder can have a suitable band gap for photocatalytic degradation of organic pollutant under visible light irradiation.

3.2 Photocatalytic degradation of CR dye by $ZrO_2/Fe_2O_3/Al_2O_3$ photocatalyst

The batch reactor was filled with CR dye solution mixed with both calcined (700°C & 800°C) and uncalcined photocatalysts. The mixture was kept for 3 hours to allow attaining adsorption equilibrium of dye on the photocatalysts. At 20 min interval, 5 mL of the sample was taken from the reactor, centrifuged at 3000 rpm for 5 min, filtered to avoid the catalyst particles and finally the absorbance of the collected samples were measured using UV-Vis spectrophotometer.

Photocatalytic degradation of CR dye was carried out both under UV and solar irradiations. The percent degradation was calculated using the following equation,

$$(\%)\ \textbf{Degradation} = \frac{(Co-Ct)}{Co}\ X\ 100 \text{..... (3)}$$

Where, C_o is the initial concentration of CR which is 50 ppm

C_t is the concentration of CR at time in minutes

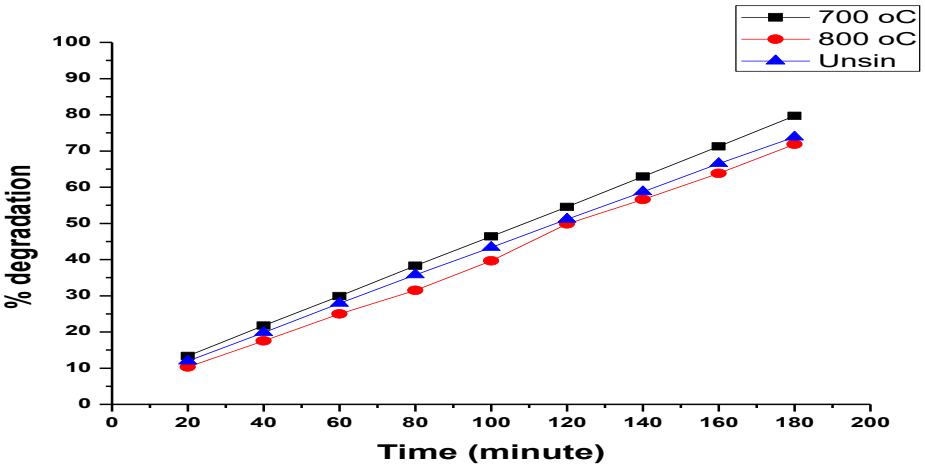

Figure 5: Percentage degradation of CR dye over the as-synthesized photocatalysts under UV- irradiation.

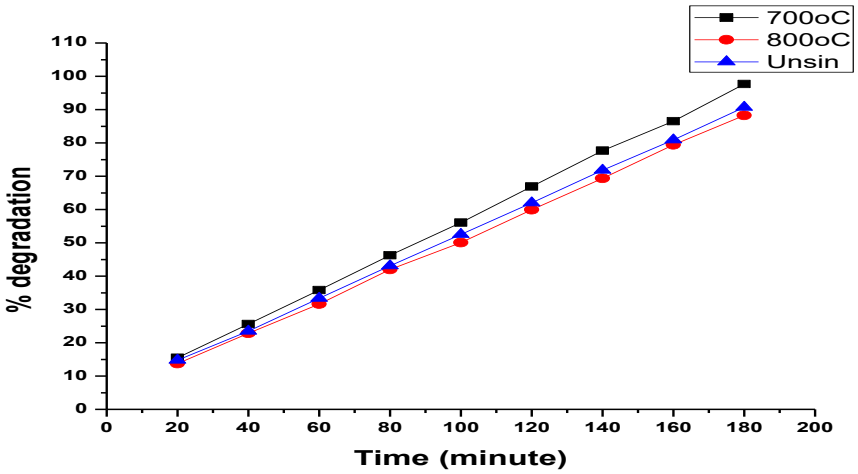

Figure 6: Percentage degradation of CR dye over as-synthesized photocatalysts under solar irradiation.

Photocatalytic degradation at 180 minute using both sintered and unsintered $ZrO_2/Fe_2O_3/Al_2O_3$ photocatalysts were carried out under UV and solar irradiations are given in figure (5) and (6)respectively. The experimental percent degradation based on equation (3)results show that when the dye solution was exposed to UV and visible light irradiation for 180 min in the presence of $ZrO_2/Fe_2O_3/Al_2O_3$ photocatalyst, about 79.72 and 97.68% of the CR dye could be degraded by UV and visible light irradiations, respectively. Accordingly, such percent degradation of the as-synthesized photocatalysts are highly active under solar than UV irradiation, this may be due to the fact that the band gap absorption edge of $ZrO_2/Fe_2O_3/Al_2O_3$ shifts to visible light. The enhanced visible light absorption can increase the number of photo-induced electrons and the formation of the superoxide (O_2 ▪) and hydroxyl radicals (OH ▪) those active species initiating a photocatalytic reaction [31-32].

3.3 Kinetic studies of photocatalytic degradation of CR dye

The kinetic studiescan be used to describe the relationship between the rates of the photocatalytic degradation of CR dye in the presence of $ZrO_2/Fe_2O_3/Al_2O_3$ photocatalyst as a function of irradiation time[33]. Plotting the natural logarithm of the ratio between the original concentration of CR and the concentration after photocatalytic degradation $\ln(C_o/C_t)$ versus the corresponding irradiation time (min) yields a linear relationship as shown in figure(7). Therefore, the photocatalytic degradation reaction of CR dye by $ZrO_2/Fe_2O_3/Al_2O_3$ belongs to the pseudo-first-order reaction kinetics. The rate constant is the slope of the straight line in figure(7). The adsorption and its photocatalytic degradation of CR dye under UV and Visible irradiations follow the pseudo first- order reaction kinetics expressed by the equation (4),

$$Kt = \ln\left(\frac{Co}{Ct}\right) \ldots\ldots\ldots\ldots\ldots\ldots (4)$$

Where:k_t is the reaction rate constant, C_o is the initial concentration of CR dye solution and C_t is the concentration of CR dye solution at the reaction time t.

The adsorption rate constant for CR dye using $ZrO_2/Fe_2O_3/Al_2O_3$ photocatalyst under the UV and visible light irradiations under the same phtocatalyst were found to be 8.3×10^{-3} and 1.66×10^{-2} min^{-1}, respectively. Correlation coefficients (R^2) of the pseudo-first order reaction under UV and visible light irradiations were found to be 0.9601 and 0.7928, respectively. The correlation coefficients for the pseudo-first- order-kinetics under UV are closer to unity than that of the visible light irradiation. In all the conditions studied, the pseudo- first-order equation did fit well to the whole range of contact times.

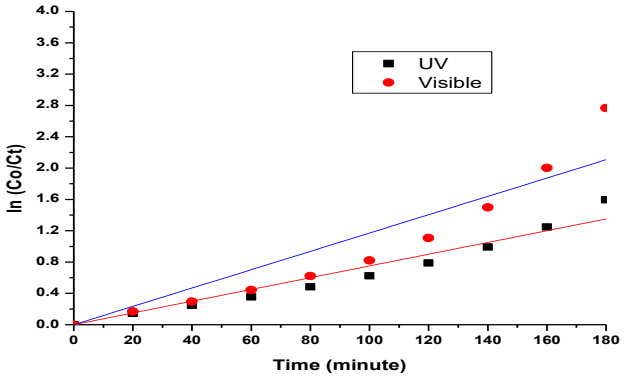

Figure 7: Plots of ln (C_o/C_t) vs. time for adsorption and photocatalytic degradation of CR dye in the presence of photocatalyst under UV and Visible light irradiations.

4 Conclusion

The Sol-gel synthesis is used as an effective method for the synthesis of $ZrO_2/Fe_2O_3/Al_2O_3$ nanoparticle and was characterized by XRD, Uv-Visible spectrophotometer, SEM-EDAX and FT-IR spectrophotometric techniques. XRD study indicate the selective stabilization of the tetragonal phase of zirconia and It can be concluded that calcinations temperature promotes crystalline of the materials as is evidenced from the XRD patterns of the samples. UV-Vis study indicates the band gap energy of the material.Its band gap energy was about 2.267 eV, which is an important band gap for improving photocatalytic degradation of organic dyes in the visible region. SEM study indicate the material to be porous and of low density. Numerous macro-pores are found to be present on the surface of the particles formed due to the escaping gases. The photocatalaytic activity of the materials was tested using CR dye as a model pollutant. The mixed photocatalyst obeyed Pseudo first order kinetics and photocatalysts sintered at 700^{o}C can act as a very good adsorbent for the removal of Congo red dye from aqueous solutionunder visible light irradiation in the presence of the catalyst.

5 Acknowledgement

The author is thankful to Research & Dissemination Directorate Office (RDO) of Dilla University for financial assistance.

6 References

1. Buitron C.L., Quezada M. and Moreno G. *Bio-resource Technology*, 92,143–149, (2004).
2. Sokmen M., Allen D.W., Akkas F., Kartal N. and Acar F. *Water Air, Soil Pollution*, 132, 153–163, 2001.
3. Sauer T., Nero G.C., Jose H.J. and Moreira R.F.P.M. *Journal of Photochemical*,149, 147, (2002).
4. Vikrant Sarin, K.K. Pant, *Bio-resource Technology*, 97, 15-20, (2006).
5. Parra,S.,Sarria, V., Maloto, S., Periner,P.and C. pulgarin,B., *journal of Environmental*, 51, 107-116, (2004).
6. Lee,K., N.H. Lee, S.H. Shin, H.G. Lee, S.J. Kima, *Material Science Engineering B*, 129, 109–115, 2006.
7. Chenthamarakshan,C.R.,K. Rajeshwar and E.J. Wolfrum, *Langmuir*, 16(6), 2715-2721, 2000.
8. Leland,J. K.,AJ Bard,*Journal of Phys. Chem*. 91:5076-5083, (1987).
9. Zhao,S.,Wu HY, L. Song, O. Tegus, S. Asuha,*Journal of MaterialSci*ence, 44:926-930, (2009).
10. 10.Bharathi,S., D. Nataraj, D. Mangalaraj, Y. Masuda, K. Senthil, K. Yong,*J. appl. Phy*.43:015-501 9p, (2010).
11. 11. Rhoton, FE, JM. Bigham, DL. Lindbo,*Appl. Geochem.*17:409-419, (2002).
12. Lei,J., C. Liu, F. Li, X. Li, S. Zhou, T. Liu, M. Gu, Q. Wu, *Journal of Hazard. Mater. B.*, 137:1016-1024, (2006).
13. Wang, YC, S. Liua, Li FB, Liu CP, JB. Liang,*J. Hazard. Mater.*162:716-723, (2009).
14. L. Ji, J. Lin, K. Ltanand C. Zeng, *Journal of Material Chemistr*y, 931-939, 2011.
15. Su C L, Li J R, He D H, *Applied Catalysis A*,202, 81,2000.
16. Wong,MS.,DM. Antonelli, JY. Ying, *Nanostructure Material*, 9: 165, 1997.
17. He, YJ, L. Winnubst, AJ. Burggraaf, *Journal of America Ceramic Soc*, 79: 3090, 1996.
18. Cullity, B.D. and Stock, S. R., *Elements of X-ray Diffraction, second ed., (Notre Dame, Addison-Wesley*, 1998).
19. Aruna, S. T. and K.S. Rajam, *Mater. Res. Bull.*, 39: 157–167, 2004.
20. Gleiter, H., *ActaMater*. 48: 1–29, (2000).
21. Nalwa, H. S., *Nanostructured Materials and Nanotechnology* (Academic Press, San Diego, 2002).
22. Tuan,W.H., Chen,R.Z., T.C. Wang, C.H. Cheng, and P.S. Kuo, (*Eur. Ceram. Soc.*, 22: 2827–2833, (2002).
23. Kibbel,B. and A.H. Heuer,*J. Am. Ceram. Soc.*, 69: 231–236, 1986.
24. Green,D.J.,*J. Am. Ceram. Soc.*, 65: 610–614, 1982.
25. Garvie,R.C. *J. Am. Chem. Soc.*, 82: 218, (1978).
26. RamS. andMondal,A. *Appl. Surf. Sci.*, 221: 237–247, (2004).
27. Gulshan, F., Kameshima, Y., Nakajima, A. and Okada, K., *Journal of Hazardous Materials*, 169: 697–702, 2009.
28. 28. Li FB, Li XZ, Liu CS,Liu TX,*J. Hazard. Mater.*, 149:199-207, 2007.
29. Chien-Tsung,W.,*J. Non-Cry. Solids*, 353:1126-1133, 2008.

30. Scheithauer,M., R. K. Grasselli, H. Knzinger, *Langmuir* 14, 3019, 1998.
31. Ihara T., M Miyoshi. Y Iriyama.,O.Matsumoto, and S. Sugihara,*Applied Catalysis B.*, 42:403-409, 2003.
32. Gole,J.L.,J. D. Stout, C. Burda, Y. Lou, and X. Chen, *Journal of PhylChemB.*, 108: 1230–1240, 2004.
33. Houas,A. H. Lachheb, M. Ksibi, E. Elaloui, C. Guillard and J. Herrmann, *Appl. Catal. B:Environ*,31, 145–157, (2001).